Characterization of the dynamic behavior of neural activity in Alzheimer's disease: exploring the non-stationarity and recurrence structure of EEG resting-state activity

Pablo Núñez[1,2], Jesús Poza[1,2,3], Carlos Gómez[,21], Verónica Barroso-García[1,2], Aarón Maturana-Candelas[1,2], Miguel A. Tola-Arribas[2,4], Mónica Cano[5], Roberto Hornero[1,2,3]

[1] Biomedical Engineering Group, University of Valladolid, Valladolid, Spain
[2] Centro de Investigación Biomédica en Red en Bioingeniería, Biomateriales y Nanomedicina (CIBER-BBN, Spain)
[3] IMUVA, Instituto de Investigación en Matemáticas, University of Valladolid, Spain
[4] Department of Neurology, Río Hortega University Hospital, Valladolid, Spain
[5] Department of Clinical Neurophysiology, Río Hortega University Hospital, Valladolid, Spain

E-mail: pablo.nunez@gib.tel.uva.es

Abstract. *Objective.* Mild cognitive impairment (MCI) and dementia due to Alzheimer's disease (AD) have been shown to induce perturbations to normal neuronal behavior and disrupt neuronal networks. Recent work suggests that the dynamic properties of resting-state neuronal activity could be affected by MCI and AD-induced neurodegeneration. The aim of the study was to characterize these properties from different perspectives: (i) using the Kullback-Leibler divergence (KLD), a measure of non-stationarity derived from the continuous wavelet transform; and (ii) using the entropy of the recurrence point density ($ENTR_{RR}$) and the median of the recurrence point density (MED_{RR}), two novel metrics based on recurrence quantification analysis. *Approach.* KLD, $ENTR_{RR}$ and MED_{RR} were computed for 49 patients with dementia due to AD, 66 patients with MCI due to AD and 43 cognitively healthy controls from 60-s electroencephalographic (EEG) recordings with a 10-s sliding window with no overlap. Afterwards, we tested whether the measures reflected alterations to normal neuronal activity induced by MCI and AD. *Main results.* Our results showed that frequency-dependent alterations to normal dynamic behavior can be found in patients with MCI and AD, both in non-stationarity and recurrence structure. Patients with MCI showed signs of patterns of abnormal state recurrence in the theta (4-8 Hz) and beta (13-30 Hz) frequency bands that became more marked in AD. Moreover, abnormal non-stationarity patterns were found in MCI patients, but not in patients with AD in delta (1-4 Hz), alpha (8-13 Hz), and gamma (30-70 Hz). *Significance.* The alterations in normal levels of non-stationarity in patients with MCI suggest an initial increase in cortical activity during the development of AD. This increase could possibly be due to an impairment in neuronal inhibition that is not present during later stages. MCI and AD induce alterations to the recurrence structure of cortical activity, suggesting that normal state switching during rest may be affected by these pathologies.

Keywords: Alzheimer's disease, mild cognitive impairment, non-stationarity, recurrence structure, wavelet analysis, recurrence quantification analysis

Submitted to: *J. Neural Eng.*

1. Introduction

The human brain is an intricate system comprised of a network of neurons that engage in a vast number of ongoing chemical and electrical processes where neural ensembles come together and disband continuously [1, 2]. Recently, a shift in the understanding of resting-state brain activity has occurred. It is now predominantly believed that the brain remains in an intrinsically active and organized state while waiting for incoming stimuli, instead of remaining in an inactive state [3]. Neural ensembles in the brain are constantly engaged in multiple interactions during rest, with neuronal activity in different brain regions dynamically changing at variable time scales [2].

Dementia due to Alzheimer's disease (AD) is a neurodegenerative pathology characterized by the perturbation of normal neural activity patterns and dynamics [1, 4]. Mild cognitive impairment (MCI) is usually considered a prodromal stage of AD [5]. The cognitive decline in people who develop dementia due to AD can be very subtle at first. This means that the distinction between normal aging and MCI, as well as the transition between MCI and AD can become blurred [5]. Consequently, and since many patients with MCI progress to AD at a later stage, it has been proposed to interpret MCI and dementia due to AD as a continuum [5]. A set of diagnostic criteria has been established to distinguish between normal aging, MCI and AD [5]. It has been reported that patients with MCI show subtle abnormal patterns of local neuronal activation compared to healthy controls, which could be an early indicator of neuronal degeneration leading to AD [6, 7]. An accurate characterization of MCI is essential in order to achieve an early diagnosis of AD.

MCI and dementia due to AD have been studied with many whole-brain imaging methods [8]. EEG is a low-cost imaging method widely used in clinical settings that measures the electrical activity generated by the synchronized firing of cortical neurons [6]. Furthermore, its high temporal resolution enables direct characterization of spontaneous cortical oscillatory activity and potentially fast brain dynamics [9]. EEG has already proven its usefulness to characterize brain dynamics [4], thus making it an ideal tool for studying alterations to normal brain dynamics during rest.

Many of the measures previously applied to EEG resting-state recordings in order to characterize its properties are derived from Fourier analysis, which entails the assumption of stationarity of the data. This limitation could lead to spurious results when overlooked [10]. EEGs are inherently non-stationary, especially in the time windows needed for the characterization of spontaneous oscillatory activity [11]. In the present study, we addressed the characterization of the dynamic properties of EEG activity by means of two distinct methodologies robust against the aforementioned limitations: wavelet analysis [12] and recurrence quantification analysis (RQA) [10]. The former allows the analysis of the time evolution of frequency patterns with optimal time-frequency resolution [12]. The latter is able to analyze recurrence plots (RPs) which enables the extraction of properties related to the dynamic behavior of a system [10]. These properties were selected in order to be able to characterize dynamic neuronal interactions, following the notion of rest as an intrinsically active state [3].

This research work is based on two preliminary studies. In one of them, we applied wavelet-based Kullback-Leibler divergence (KLD) to a small database of 18 healthy controls, 10 patients with MCI and 32 patients with dementia due to AD. We found that the level of non-stationarity during rest in the 1-70 Hz frequency range increased with the severity of the disease [13]. In another work, we used *TREND*, a RQA-based measure, to evaluate dynamic neuronal patterns in healthy controls and patients with AD. We found that AD induced a frequency-dependent pattern of alterations in EEG activity during rest [14]. However, *TREND* only measures drifts or trends in non-stationary processes [15], which limits its usefulness to characterize the dynamic behavior of the recurrence structure of the EEG. In the present study we aim to overcome the limitations of these past works. To this end, we performed an in-depth analysis of wavelet non-stationarity and applied two novel RQA measures able to characterize the unpredictability and sparsity of the recurrence structure.

The main hypothesis of the present study was that the MCI-AD continuum induces a frequency-dependent pattern of alterations to the dynamic properties of single-channel resting-state EEG activity. These include non-stationarity, as well as the density and unpredictability of its recurrence structure. We also hypothesized that approaching these properties by means of different methods (time-frequency analysis and RQA) could reveal different alterations of brain dynamics and give a better understanding of the disease-induced abnormalities in cortical oscillatory activity.

To test this hypothesis, three measures were computed. The first one was KLD, derived from the continuous wavelet transform (CWT), which is able to assess the level of non-stationarity of the system. KLD has proven its usefulness to successfully estimate EEG non-stationarity and characterize transient abnormal frequency-dependent activation patterns [16, 17]. The other two were novel RQA measures: the entropy of the recurrence point density ($ENTR_{RR}$, which measures

the unpredictability of the recurrence structure of a system) and the median of the recurrence point density (MED_{RR}, which measures the density of the recurrence structure, *i.e.* how recurrent a system is). Specifically, we will try to answer the following research questions: (i) do the level of non-stationarity and the recurrence structure of the EEG reveal frequency-dependent alterations in patients with MCI and AD?; (ii) can different approaches to the characterization of the dynamic properties of the EEG reveal complementary information about disease-induced abnormalities?; (iii) do the alterations to EEG non-stationarity, recurrence unpredictability and recurrence density reflect the progression of dementia?

2. Materials

2.1. Subjects

The study sample was formed by 158 subjects: 43 cognitively healthy controls, 66 patients with MCI due to AD and 49 patients with dementia due to AD. The criteria of the National Institute on Aging and Alzheimer's Association (NIA-AA) were followed to diagnose patients with MCI or dementia due to AD [18, 19]. The control group was composed of elderly subjects with no history of neurological or psychiatric disorders. The following exclusion criteria were used: (1) history or presence of another psychiatric or neurological disease; (2) uncommon clinical presentations or atypical course according to the NIA-AA criteria; (3) advanced dementia (Clinical Dementia Rating = 3); (4) institutionalized patients; and (5) medication that could affect EEG activity. The socio-demographic characteristics of each group are shown in Table 1.

All participants and caregivers were informed about the research and study protocol and gave their written informed consent. The study was approved by the Ethics Committee of the Río Hortega University Hospital (Valladolid, Spain) according to the Code of Ethics of the World Medical Association (Declaration of Helsinki).

2.2. Electroencephalographic recordings

EEG signals were recorded by means of a 19-channel EEG system (XLTEK®, Natus Medical) at the Department of Clinical Neurophysiology of the Río Hortega University Hospital, Valladolid, Spain. EEG activity was recorded following the specifications of the international 10-20 system from electrodes Fp1, Fp2, Fz, F3, F4, F7, F8, Cz, C3, C4, T3, T4, T5, T6, Pz, P3, P4, O1, and O2, at a sampling frequency of 200 Hz. The signals were re-referenced by means of common average referencing. Subjects were asked to remain with their eyes closed, still and awake during the acquisition of the EEG. In order to prevent sleepiness, EEG traces were visually monitored on real time and subjects were asked to remain awake if signs of drowsiness were found. Drowsiness episodes, eye-movement related artifacts and muscle activity were identified and marked during the course of the EEG recordings.

Five minutes of EEG activity were recorded for each subject. They were preprocessed in three steps [20]: (i) preliminary independent component analysis to remove components related to artifacts; (ii) finite impulse response filtering (Hamming window, filter order 2000, forward and backward filtering) to remove 50 Hz noise power and to limit spectral content to the wide frequency band of [1 70] Hz; and finally (iii) visual rejection of the remaining artifacts, selecting the first 60 consecutive seconds without noise contamination for each subject.

3. Methods

Three measures were computed from the artifact-free 60-s EEG recordings: KLD, $ENTR_{RR}$ and MED_{RR}. The three measures were computed on 10-second epochs by means of a sliding window technique with no overlap [14]. KLD was computed from the CWT of each 10-s epoch, while $ENTR_{RR}$ and MED_{RR} were derived from the RP of each 10-s segment. All three measures were computed in the conventional frequency bands: delta (δ, 1-4 Hz), theta (θ, 4-8 Hz), alpha (α, 8-13 Hz), beta-1 ($\beta 1$, 13-19 Hz), beta-2 ($\beta 2$, 19-30 Hz) and gamma (γ, 30-70 Hz), as well as in the global (1-70 Hz) frequency band. The 60-s recordings were filtered in the frequency bands under study before the computation of the RPs, by means of FIR filters (Hamming window, filter order 2000, forward and backward filtering).

KLD measures the level of non-stationarity of each EEG segment and its computation is described in section 3.1. $ENTR_{RR}$ and MED_{RR} quantify the unpredictability of the recurrence structure and the recurrence density of each EEG segment, respectively. Their computation is described in section 3.2.

After computation, all measures were averaged across epochs, thus reducing the data to 19×7 (electrodes $\times$ frequency bands) matrices for each subject.

3.1. Time-frequency analysis

The implementation of KLD in the present study is based on the time-frequency analysis. This term encompasses a variety of methods and techniques that aim to capture temporal information about the spectral content of the EEG [21]. These

Table 1. Socio-demographic and clinical data. AD: Alzheimer's disease; MCI: mild cognitive impairment; m: median; IQR: interquartile range; M: male; F: female; A: primary education or below; B: secondary education or above; MMSE: Mini-Mental State Examination.

Data	Group		
	Controls	Patients with MCI	Patients with AD
Number of subjects	43	66	49
Age (years) (m[IQR])	75.8[74.0, 78.7]	77.3[72.6, 80.7]	79.1[75.8, 82.4]
Sex (M:F)	13 : 30	29 : 37	22 : 27
Education level (A:B)	16 : 27	40 : 26	35 : 14
MMSE (m[IQR])	29.0[28.0, 30.0]	27.0[26.0, 28.0]	22.0[19.3, 23.3]

methods are based in the decomposition of the EEG into time-frequency representations (TFR). They provide information about neural synchrony that is not apparent in the ongoing EEG, including which frequencies display the most power at specific time points [21]. These power shifts are often assumed to reflect underlying changes in neural synchrony, which makes time-frequency-derived measures useful to assess variations in dynamic properties of the EEG, such as non-stationarity [17]. Furthermore, they do not assume stationarity, as opposed to traditional spectra-based frequency analysis [17].

There are different methods to estimate a TFR for time-frequency analyses, such as the short-time Fourier transform (STFT) or the Hilbert transform. In general, longer time windows provide higher frequency resolution and lower temporal resolution, which is a limitation of the STFT. An alternative method is the CWT. The CWT is conceptually related to the STFT [22], but it is more adequately suited to the study of EEG dynamics. The CWT overcomes the aforementioned trade-off between time and frequency resolution [23]. Wavelet analysis allows flexible control over the resolution, facilitating the localization of neuroelectric components and events in time and frequency [24]. For this reason, the CWT was chosen to estimate the TFR in the present study.

3.1.1. Continuous wavelet transform (CWT). Several parameters need to be adjusted for the computation of the CWT. In this study the Morlet wavelet was used as mother wavelet, as it is a biologically plausible fit to the EEG signal [21]. The parameters center frequency and bandwidth were set to 1 in order to achieve an adequate balance between the time (Δt) and frequency resolution (Δf) at low frequencies [25]. The width of the Heisenberg box was chosen to be two times Δt and Δf as a tradeoff between temporal and frequency resolution [25].

The computation of the CWT over a finite-time length series results in errors at the beginning and end of the wavelet power spectrum. To overcome this limitation, zero padding is introduced at the beginning and end of the epoch [26]. However, this introduces discontinuities at the edges where the CWT computation is unreliable. To overcome this problem, the cone of influence (COI) was taken into account when computing KLD. The COI is the region of the wavelet spectrum in which the edge effects can be ignored [26], thus avoiding the distortions introduced by zero padding. KLD (described in section 3.1.2) was computed from the CWT of each EEG epoch.

3.1.2. Kullback-Leibler divergence. Considering an EEG time series $x(t) = \{x_1, x_2, \ldots, x_N\}$, let $tfr(f_i, n\Delta t)$ be its CWT scalogram (square of the absolute value of the CWT) at each frequency f_i and time point $n\Delta t$. The marginal frequency distribution $tfr(f_i)$ can be computed as follows:

$$tfr(f_i) = \frac{1}{N} \sum_{n=1}^{n=N} tfr(f_i, n\Delta t). \quad (1)$$

Afterwards, the temporal TFR distribution $p_{f_i,n\Delta t}$ is calculated:

$$p_{f_i,n\Delta t} = \frac{1}{N} \frac{tfr(f_i, n\Delta t)}{tfr(f_i)}. \quad (2)$$

KLD measures the discrepancy between two distributions $p_{f_i,n\Delta t}$ and $q_{f_i,n\Delta t}$ and is calculated as follows [17]:

$$KLD(f_i) = \sum_{n=1}^{n=N} \log_2 \frac{q_{f_i,n\Delta t}}{p_{f_i,n\Delta t}}. \quad (3)$$

In this implementation of KLD, $q_{f_i,n\Delta t}$ corresponds with a uniform distribution in the time domain $\{q_{f_i,n\Delta t} = q_0 = 1/N\}$. If the signal is stationary, $tfr(f_i, n\Delta t)$ is constant at each f_i (*i.e.*, $tfr(f_i, n\Delta t) = tfr(f_i)$, that is, $tfr(f_i, n\Delta t)$ has the same value for any $n\Delta t$. This would result in $KLD(f_i) = 0$). KLD will increase as the signal becomes less stationary at a given frequency f_i [16]. Thus, KLD can be interpreted as an indicator of the non-stationarity of the TFR. KLD was computed by means of the CWT in the [1 70] Hz frequency range and then averaged in the frequency bands under study, with the COI being applied to the wavelet beforehand.

3.2. Recurrence plots

Recurrence ('returning to previous states') is a fundamental property of many dynamical systems in a variety of areas of research, including economics, population dynamics, meteorology and brain dynamics [15]. RPs are two-dimensional plots that represent a binary symmetric square recurrence matrix and help to visualize the periodicity patterns of such dynamical systems [15, 27, 28].

Considering a scalar and discrete EEG time series $x(t) = \{x_1, x_2, \ldots, x_N\}$, the multidimensional process of $x(t)$ as a trajectory in m-dimensional phase space $\boldsymbol{X}_i$ can be reconstructed by means of the time delay method [15]:

$$\boldsymbol{X}_i = \sum_{k=1}^{m} x_{i+(k-1)\tau} \vec{e}_k, \tag{4}$$

where m is the embedding dimension and τ is the time delay. $\vec{e}_k$ are unit vectors spanning an orthogonal coordinate system. In their original definition, RPs are symmetric $N \times N$ binary arrays [15]:

$$\mathbf{R}_{i,j}(\varepsilon) = \Theta(\varepsilon - \|\boldsymbol{X}_i - \boldsymbol{X}_j\|), \tag{5}$$

where ε is a threshold, $\Theta(\cdot)$ is the Heavyside function and $\|\cdot\|$ is a norm (in this case the commonly used Euclidean norm [15, 28]). An overly large ε will cause artifacts, while a small ε will lead to a lack of recurrence points [15]. Thus, the threshold ε must be carefully selected. It has been shown that for EEG data, a rule of thumb for the threshold selection is 0.25 of the standard deviation of the data [29]. Examples of the computation of RPs from an EEG epoch can be seen in figure 1.

The embedding parameters delay (τ) and dimension (m) need to be chosen carefully [15]. These parameters were optimized in a previous work [14]. Specifically, they were optimized by means of the widely used mutual information function and the nearest neighbors algorithm [15], respectively, for each frequency band under study. The delay τ was set to 22 samples for the delta band, 8 samples for the theta band, 5 samples for the alpha band, 3 samples for the beta-1 and beta-2 bands and 4 samples for the gamma band [14]. The embedding dimension m was set to 4 for all bands [14]. An embedding dimension of 4 might seem small for physiological data time series, such as EEG. However, other studies analyzing EEG recordings by means of RPs have used a variety of values for m, ranging from 3 to 11 [29, 30, 31]. All these studies used the mutual information and nearest neighbors algorithm to optimize τ and m. This suggests that these values are highly dependent on the sampling frequency and length of the epochs from which RPs are computed [28]. Moreover, EEG recordings are inherently noisy, and an overly high embedding dimension will amplify this noise to the detriment of real dynamics [10], which further supports our obtained value of $m = 4$.

The embedding parameters m, τ and ε were fixed for every subject in order to ensure fair comparisons between subjects, even though in an inherently dynamic system, such as the EEG, these parameters might change with time and for each subject. This way, the RPs were constructed from a common phase space [28].

3.2.1. Recurrence quantification analysis. RQA encompasses a series of techniques and strategies aimed at objectively characterizing RPs by means of descriptive variables [10]. RQA allows the quantification of the small scale structures in RPs [15]. RQA measures can be applied directly to a global sequence, but a windowed application of RQA, such as the one used in the present study, enables the observation of changes in the autocorrelation structure of the series over time [10]. Different small-scale structures can be observed in RPs. The main ones are: single recurrence points (when states are rare or fluctuate strongly [15]), diagonal lines (when a segment of the trajectory in phase space runs almost in parallel to another [15]), and vertical lines (a time interval in which the state does not change [15]).

RQA measures can be based on the recurrence density, on diagonal lines, or on vertical lines [32]. RQA measures based on diagonal structures were chosen for this study as they have the advantage of being less sensitive to embedding than those based on vertical ones [32]. Many RQA measures based on diagonal structures have been proposed: the ratio of diagonal lines in the RP (DET), which has been interpreted as a measure of the predictability of the system [15]; the average diagonal line length (L), which represents the mean prediction time [15]; and the Shannon entropy of the probability of finding diagonal lines of exactly length l ($ENTR$), which has been said to reflect the diagonal complexity of the RP [15], among others. Another subset of these RQA measures are those based on the distance to the main diagonal (line of identity, LOI). These include DET_τ (the proportion of diagonal lines to all recurrence points) and L_τ (the mean length of the diagonal structures on each diagonal parallel to the LOI) [15]. In particular, the τ-recurrence rate for the diagonal lines with distance τ from the LOI (recurrence point density) is defined as [15]:

$$RR_\tau = \frac{1}{N-\tau} \sum_{i=1}^{N-\tau} \mathbf{R}_{i,i+\tau}. \tag{6}$$

This measure can be considered as a generalized autocorrelation function and can be seen as the probability that a state recurs to its ε-neighbourhood after τ

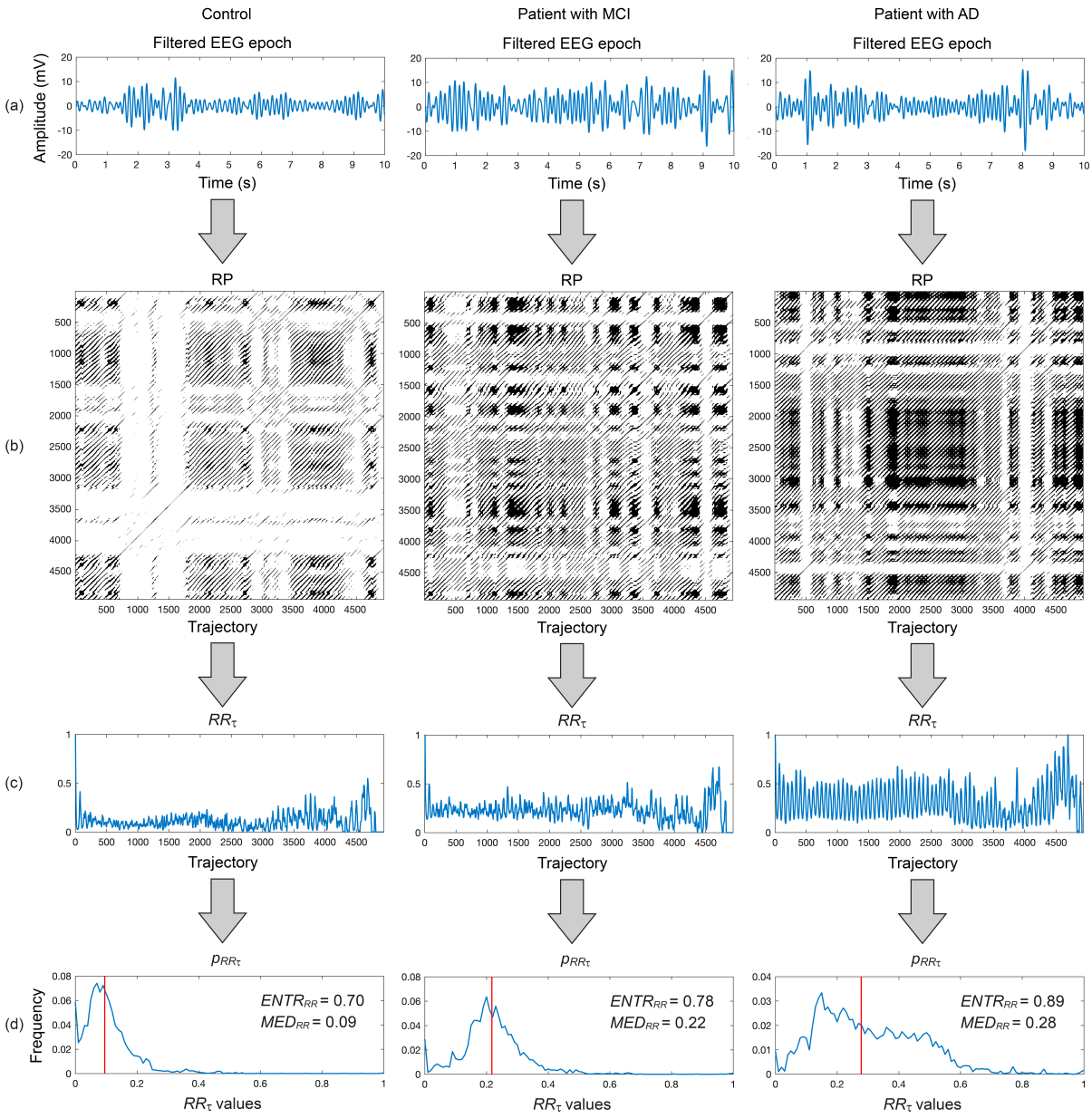

Figure 1. Computation of $ENTR_{RR}$ and MED_{RR} for a representative subject from each group (C, MCI and AD). Panel (a) shows a 10-s EEG epoch filtered in the theta band (Pz channel). Panel (b) displays the RP computed from the EEG epochs in (a), while panel (c) shows the corresponding recurrence point density (RR_τ). Finally, panel (d) displays the probability density function (p_{RR_τ}) of RR_τ in panel (c). The red line corresponds to MED_{RR}, while $ENTR_{RR}$ is computed from p_{RR_τ}.

time steps [15]. The main measure based on RR_τ is $TREND$, which provides information on the non-stationarity of a process [15].

Many of the measures based on diagonal lines have limitations that prevent them from fully characterizing the dynamic behavior of the EEG. For the computation of DET, $ENTR$ and L one has to establish a threshold for the minimum diagonal size, which is not trivial and could decrease its reliability [15]. Furthermore, while $TREND$ is able to characterize the non-stationarity of the system, it is better suited to characterize drifts or trends due to its nature as a linear regression coefficient over RR_τ [15]. Drifts or trends are only a subset of possible non-stationarities, thus limiting the ability of KLD to characterize non-stationary EEG epochs.

In this study we have introduced two novel measures based on RR_τ that overcome the aforementioned limitations. The first one, $ENTR_{RR}$, is able to characterize the the unpredictablity of the recurrence structure of the EEG epoch. The second one, MED_{RR}, is

able to characterize the density of the RP, and gives a general idea on the degree of recurrences of an EEG epoch (i.e., how often it returns to previous states). Both $ENTR_{RR}$ and MED_{RR} were calculated by first FIR filtering the whole 60-s segments in the frequency bands and then conducting the RQA analysis described in the following sections on the 10-s epochs for each band (see figure 1).

3.2.2. Entropy of the recurrence point density. The entropy of the recurrence point density ($ENTR_{RR}$) characterizes the unpredictability of RR_τ by computing the Shannon entropy of its probability distribution. This measure is a quantification of the unpredictability of state recurrence as a function of the distance τ between points in the phase space trajectory. By measuring how unpredictable RR_τ is, we can characterize its structural richness across τ [33]. For example, a low $ENTR_{RR}$ value would indicate an overall homogeneous distribution of RR_τ, while a heterogeneously distributed RR_τ would result in higher values. Thus, $ENTR_{RR}$ can be interpreted as a measure of how unpredictable the state recurrence structure of the signal is over time. $ENTR_{RR}$ can be computed as follows:

$$ENTR_{RR} = \frac{-\sum_{i=1}^{M} p_{RR_\tau}(i)\log(p_{RR_\tau}(i))}{\log(M)}, \quad (7)$$

where p_{RR_τ} is an estimation of the probability density function of RR_τ and M is the number of bins of p_{RR_τ}. In this study the number of bins was set to 100 with edges between 0 and 1 (the minimum and maximum values of RR_τ). The set number of bins was chosen to enable fair comparisons and due to the empirical observation that the optimal number for most distributions in our dataset was in the range of 90 to 100 (Freedman-Diaconis rule [34]). Figure 1 illustrates how $ENTR_{RR}$ is computed.

3.2.3. Median of the recurrence point density The other measure introduced in the current study is the median of the recurrence point density MED_{RR}. This measure provides information on the density of the RP while avoiding the effects of abnormally high or low recurrence density at specific τ values. When a signal has a high MED_{RR} it means that the system is highly recurrent (*i.e.*, it often returns to previous states). On the other hand, a low value means that the recurrence structure of the signal is sparsely populated, indicating that the system tends to not return to previous states. It can thus be seen as a less skewed version of the recurrence rate and can be interpreted as an indicator of the sparsity of the recurrence structure of the signal. Figure 1 shows the computation of MED_{RR}.

3.3. Statistical analyses

We carried out an exploratory analysis to assess the distribution of KLD, $ENTR_{RR}$ and MED_{RR}. Normality was assessed with the Lilliefors test, while homoscedasticity was assessed with the Levene test. The results showed that KLD, $ENTR_{RR}$ and MED_{RR} values did not meet parametric tests conditions. Thus, between-group differences were assessed with non-parametric tests.

We performed Kruskal-Wallis tests on the grand-average (average of all electrodes) KLD, $ENTR_{RR}$ and MED_{RR} values in each frequency band to detect global interactions between the three groups. Afterwards, Mann-Whitney U-tests were conducted to assess grand-average and spatial pairwise between-group differences for KLD, $ENTR_{RR}$ or MED_{RR} in each frequency band.

A false discovery rate (FDR) correction was used to control for type I error, [35]. FDR correction was applied to control for the number of electrodes, with a significance level of $\alpha = 0.05$. Signal processing and statistical analyses were performed using MATLAB® (version R2018a Mathworks, Natick, MA).

4. Results

4.1. Analysis of socio-demographic and clinical data

In order to assess possible differences between groups that could act as confounding factors, statistical analyses were conducted over all socio-demographic and clinical data. Subjects were matched by age ($\chi^2(2) = 5.47$, $p = 0.065$, Kruskal-Wallis test) and sex ($\chi^2(2) = 2.35$, $p = 0.309$, Chi-squared test). The subject groups were not matched by education level ($\chi^2(2) = 16.25$, $p < 0.001$, Chi-squared test). In order to test whether the mismatch could have an effect on the between-group comparisons, we tested for statistical differences in grand-average KLD, $ENTR_{RR}$ and MED_{RR} between subjects with education level A and B for all groups (Mann-Whitney U-test). No statistical differences for any of the measures in any group or band were found ($p > 0.05$).

As expected, MMSE scores were lower in patients with AD compared to controls ($U = 3.035$, $p < 0.001$, Mann-Whitney U-test) and patients with MCI ($U = 3.224$, $p < 0.001$, Mann-Whitney U-test). MMSE scores were lower in patients with MCI compared to controls ($U = 8.004$, $p < 0.001$, Mann-Whitney U-test).

4.2. Grand-average analyses

The grand-average values for KLD, $ENTR_{RR}$ and MED_{RR} over all electrodes for each frequency band are displayed in figure 2. Statistically significant

between-group differences ($p < 0.05$, Kruskal-Wallis test with FDR correction) were found for all measures in the theta (KLD: $\chi^2(2) = 15.59$, $p = 0.003$; $ENTR_{RR}$: $\chi^2(2) = 17.45$, $p < 0.001$; MED_{RR}: $\chi^2(2) = 16,74$, $p = 0.001$), beta-1 (KLD: $\chi^2(2) = 8.68$, $p = 0.019$; $ENTR_{RR}$: $\chi^2(2) = 17.49$, $p < 0.001$; MED_{RR}: $\chi^2(2) = 16.08$, $p = 0.001$) and beta-2 bands (KLD: $\chi^2(2) = 12.14$, $p = 0.008$; $ENTR_{RR}$: $\chi^2(2) = 10.71$, $p = 0.008$; MED_{RR}: $\chi^2(2) = 9.23$, $p = 0.023$). KLD also displayed statistically significant between-group differences in the delta ($\chi^2(2) = 8.18$, $p = 0.019$), alpha ($\chi^2(2) = 10.87$, $p = 0.010$) and gamma bands ($\chi^2(2) = 7.97$, $p = 0.019$). Finally, KLD and $ENTR_{RR}$ displayed statistically significant between-group differences in the global frequency band (KLD: $\chi^2(2) = 8.05$, $p = 0.019$; $ENTR_{RR}$: $\chi^2(2) = 11.39$, $p < 0.001$)

In the case of KLD, the results showed that, in the theta band, controls displayed the highest levels of non-stationarity, patients with AD had the lowest levels overall and patients with MCI were in-between. The opposite behavior was found in the beta-1 and beta-2 bands. Interestingly, in the delta, alpha and gamma bands (which only show statistically significant differences for this measure), patients with MCI displayed the lowest (alpha) and highest (delta, gamma, global) KLD values of all groups, while values for patients with AD were in-between healthy controls and patients with MCI. The post-hoc Mann-Whitney U-tests revealed that the groups were best differentiated in the theta band, where statistically significant differences were found for all pairwise comparisons. In the alpha, beta-2 and global bands, only the control group showed statistically significant differences with the other two groups, while in the delta and gamma bands only controls and subjects with MCI displayed statistically significant differences. Finally, in the beta-1 band, statistically significant differences were only found between controls and patients with AD.

The $ENTR_{RR}$ results indicated that, in the theta band, patients with AD had the most unpredictable recurrence structure, followed by patients with MCI and finally healthy controls. The opposite was observed in the beta-1 and beta-2 bands, while in the global band, the MCI group displayed the highest unpredictability in the recurrence structure of all three groups. Finally, the MED_{RR} values showed that, in the theta band, the sparsity of the recurrence structure increased with the severity of the disease. On the other hand, in the beta-1 band, the effect was the opposite. The post-hoc Mann-Whitney U-tests revealed that statistically significant differences were only found between controls and the other two groups.

4.3. Spatial analyses

Figure 3 shows topographic maps of the statistical differences ($p < 0.05$, Mann-Whitney U-test with FDR correction) in all the frequency bands under study. Comparisons between patients with MCI and subjects with AD are not shown, as no statistically significant differences between those groups were found for any of the measures.

In the delta band, MCI patients showed localized patterns of increased KLD values compared to controls in the central, frontal and left-temporal regions. The between-group comparisons in the theta band showed lower KLD and higher $ENTR_{RR}$ and MED_{RR} for patients with MCI compared to healthy controls in the frontal and parieto-occipital regions, while patients with AD displayed widespread lower KLD and higher $ENTR_{RR}$ and MED_{RR} than controls. Statistically significant differences in the alpha band were, again, only found for KLD, with MCI patients showing widespread reduced non-stationarity compared to controls. This effect was less significant in patients with AD, where the decrease in KLD compared to controls was reduced. In the beta-1 band $ENTR_{RR}$ and MED_{RR} showed similar patterns, with MCI patients having reduced values in the parieto-occipital region compared to controls and patients with AD exhibiting widespread lower values. Statistically significant differences between groups in this band were less marked for KLD, with only patients with AD having higher values in the parieto-occipital region compared to controls.

Spatial patterns were again similar for all three measures in the beta-2 band. Here, MCI patients showcased higher KLD and lower $ENTR_{RR}$ and MED_{RR} than controls in the frontal, right-temporal and parieto-occipital regions. Patients with AD also showed higher values for all three measures compared to controls. The statistically significant differences were localized in the right-temporal, parieto-occipital and left-temporal regions. In the gamma band, only MCI patients displayed higher KLD than controls in the temporal and parietal regions. Finally, in the global band, both KLD and $ENTR_{RR}$ were significantly higher in controls, with the differences being mostly localized in the left hemisphere for KLD and widespread for $ENTR_{RR}$. In order to further confirm the results, we also performed the grand-average analyses for each spatial region separately (frontal, left-temporal, right-temporal, central and parieto-occipital) and found that the results mostly followed the ones in the spatial analyses (see supplementary material, figures S1 to S5).

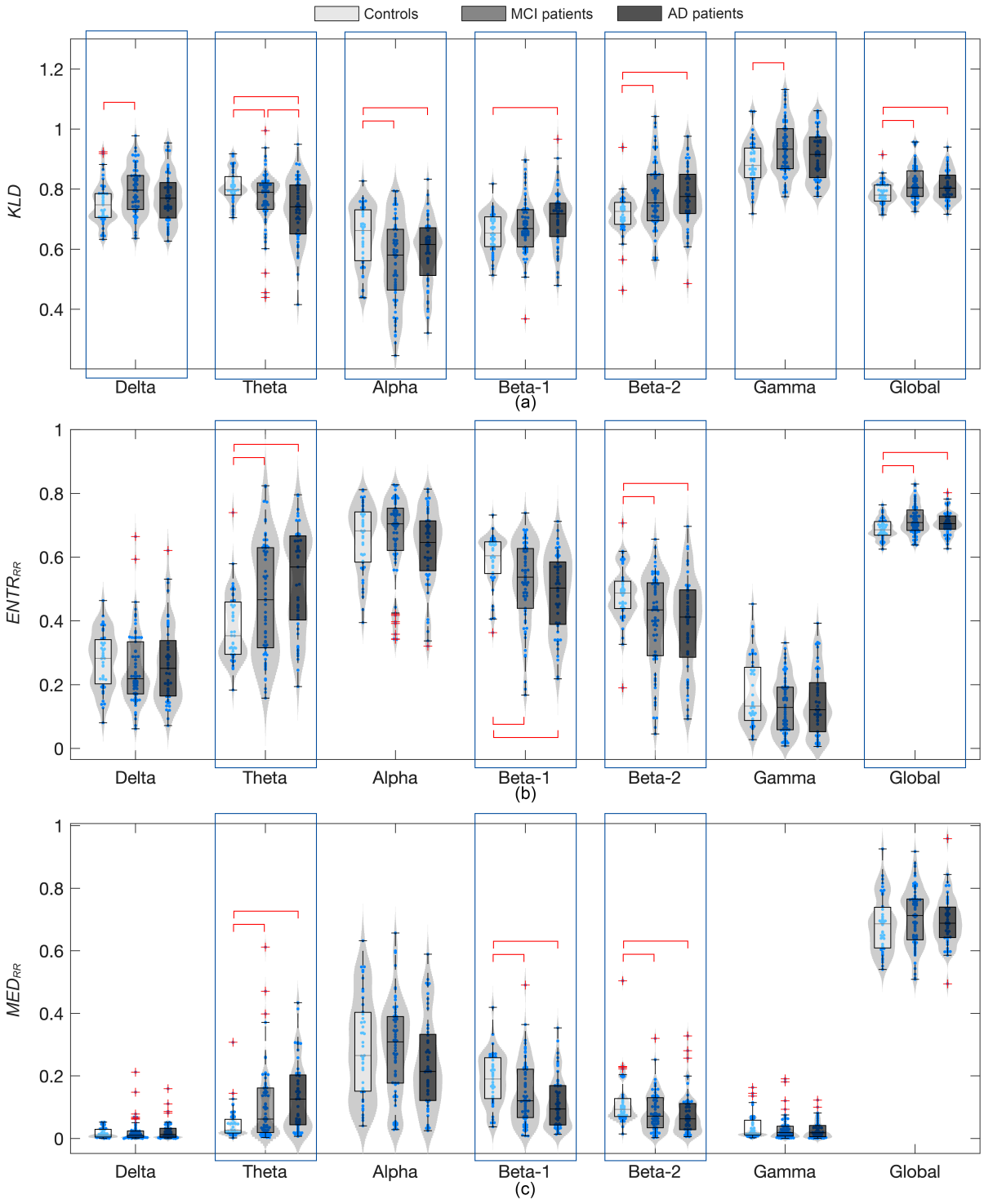

Figure 2. Distribution plots depicting normalized grand-average values for (a) KLD, (b) $ENTR_{RR}$ and (c) MED_{RR} in each frequency band under study. For each distribution plot, the lower bar represents the first quartile, the middle bar indicates the median and the top bar marks the third quartile. The whiskers mark the most extreme points not considered outliers and the red crosses represent the outliers. Statistically significant between-group differences are marked with blue rectangles ($p < 0.05$, Kruskal-Wallis test, FDR corrected p-values). Statistically significant post-hoc pairwise differences are marked with red brackets ($p < 0.05$, Mann-Whitney U-test, FDR corrected p-values).

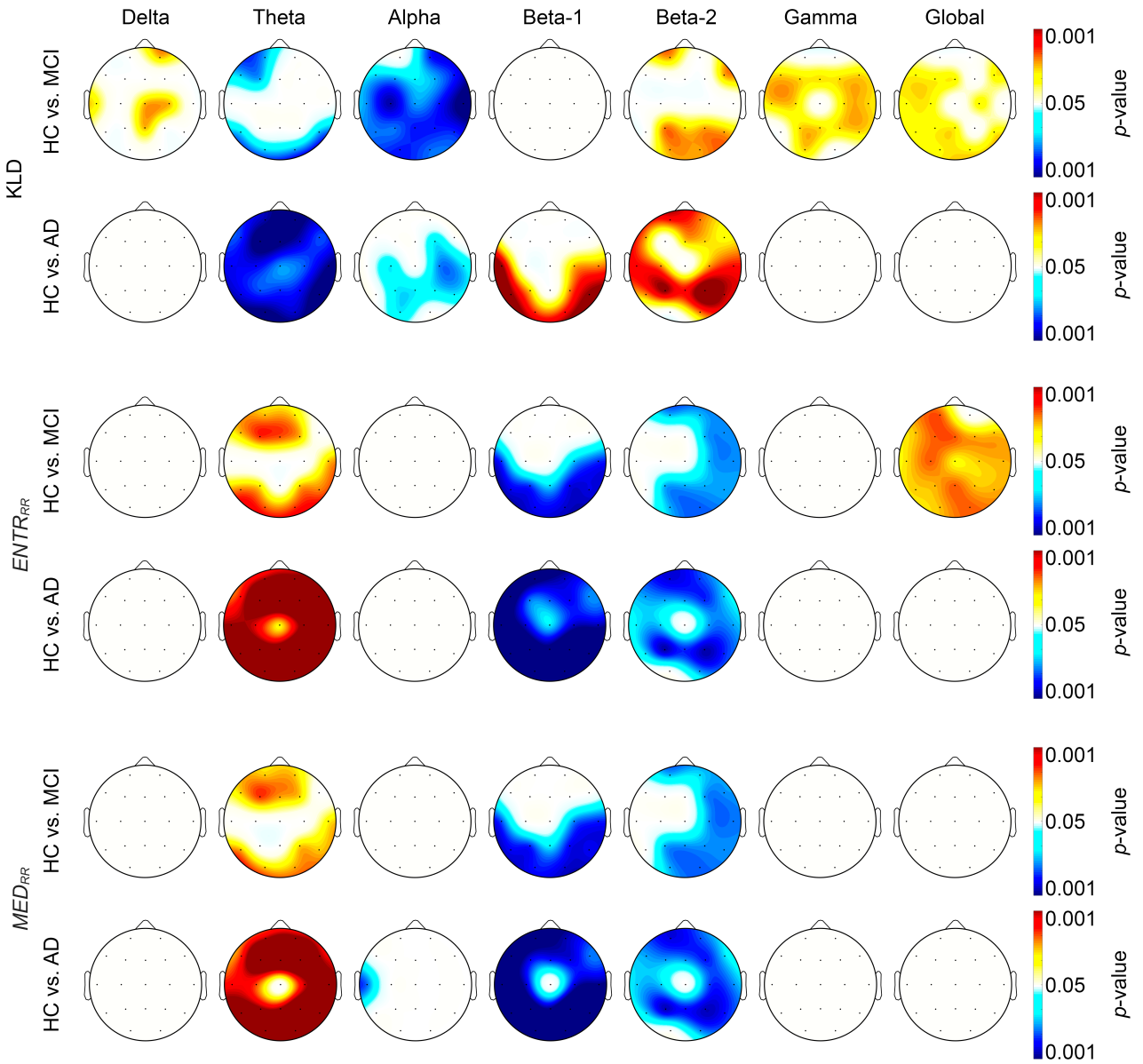

Figure 3. Topographic maps of the statistical comparisons between healthy controls and MCI patients (HC vs. MCI), and healthy controls and patients with AD (HC vs. AD) in the traditional frequency bands and the global band for KLD, $ENTR_{RR}$ and MED_{RR}. Warm colors indicate that the second group displayed statistically significant higher values than the first group ($p < 0.05$, Mann-Whitney U-test with FDR correction), while cold colors represent the opposite.

5. Discussion

In the present study, we investigated the dynamic behavior of EEG activity in healthy elderly controls, patients with MCI and with dementia due to AD by means of a set of measures based on the CWT and RQA. Our findings indicate that: (i) MCI and AD induce alterations in the level of non-stationarity, recurrence unpredictability and recurrence density; (ii) different approaches to analyze electrode-level EEG activity reveal distinct patterns of disease-induce abnormalities; (iii) the evolution of non-stationarity, recurrence unpredictability and recurrence density alterations support the notion of an MCI-AD continuum.

5.1. AD- and MCI-induced alterations of locally-activated dynamic patterns

The main hypothesis of the present study was that there is a frequency-dependent pattern of alterations in the dynamic properties of resting-state EEG activity

induced by MCI and AD. All measures showed statistically significant differences between the healthy controls and the groups affected by MCI or AD in the theta, beta-1 and beta-2 bands, while only KLD showed statistically significant abnormalities in the delta and gamma bands. Finally, both KLD and $ENTR_{RR}$ showed abnormalities in the global frequency band. Inspecting the patterns of statistically significant differences, a clear distinction can be made between the theta and beta bands. Specifically, the tendencies towards higher or lower non-stationarity, recurrence unpredictability and recurrence density are reversed in the beta bands (beta-1 and beta-2) compared to the theta band. Interestingly, the patterns in the global band follow those of the higher frequency bands for KLD and those of the lower frequency bands for $ENTR_{RR}$.

In the theta band, KLD showed a decrease in left-frontal and parietal non-stationarity in patients with MCI that extended to the whole scalp in patients with AD. On the other hand, an increase in $ENTR_{RR}$ and MED_{RR} in MCI and AD patients was observed, with similar patterns to those of KLD. This indicates that MCI and AD may induce a decrease in the non-stationarity of low-frequency cortical oscillatory activity, as well as an increase in the unpredictability and the density of the recurrence structure. These results suggest that the increase in the stationarity of the EEG activity found in pathological subjects is accompanied by both high number of recurrences, as well as a more unpredictable state recurrence structure. The latter result could seem counterintuitive in contrast to the decrease in non-stationarity, but it can be easily explained. The more non-stationary nature of the EEG activity in healthy controls induces more disruptions in the recurrence structure (diagonal bands in the RP whose value is equal to 0), thus decreasing the entropy of RR_τ. The high density of the recurrence structure means that the oscillatory activity is relatively similar to itself across time compared to that of controls, which is associated to a stationary process [15] and is in agreement with the KLD results.

The results in the theta band agree with previous studies that reported a decrease in the irregularity and variability of the neural activity of AD patients [6, 36]. It has been shown that the reduced regularity in low frequencies observed in patients with MCI and AD is correlated with the widely reported slowing of EEG activity found in those diseases [36]. A slight negative relation between KLD and relative power has been reported [16]. This fact could indicate that the decrease in theta band non-stationarity might partially be a consequence of the increase in overall power in low frequencies that occurs in MCI and AD. This would be in agreement with other studies that found that the frequency shift in dominant power for MCI patients is slightly less marked than the one found in patients with AD [6, 37]. Indeed, the KLD results in the alpha band further support this theory: as can be observed in figure 3, MCI patients displayed a widespread decrease in non-stationarity compared to controls that was much less pronounced in patients with AD.

It is commonly thought that the earliest AD-induced changes are an increase in theta and a decrease in beta activity, followed later by a decrease in alpha activity [37]. However, our results suggest that alpha activity may be increased in patients with MCI. This leads to a decrease in non-stationarity, before increasing again at a later stage. The increase in alpha activity could be seen as a compensatory mechanism of the brain that occurs in response to the loss of cognitive efficiency induced by MCI [38, 39]. However, it has also been stated that excessive neuronal activity during AD pathogenesis, which has been linked to the development of β-amyloid plaques, may not be compensatory but pathological and could induce a disruption of brain dynamics [40]. It has been proposed that the cause of the pathological increase in neural activity is due to an impairment in neuronal disinhibition [40]. This causes an increase in spike density before the slowing finally sets in [40] and may be induced by β-amyloid depositions [41]. In particular, acetylcholinesterase (AChE) has been shown to promote the aggregation of β–amyloid [42] and a deficit of cholinergic innervation has been observed in the temporal neocortex patients with MCI, which has been suggested to be an early sign of pre-dementia neurodegeneration [42]. This spiral of increasing activity could be reflected in the more stationary alpha oscillations found in MCI patients. Furthermore, there is evidence that hyperactivation in MCI may reflect early excitotoxicity [43].

In contrast to the lower frequencies, beta non-stationarity was increased in pathological subjects, with a localized increase in the parietal area for MCI patients that extended to the frontal region in patients with AD, while leaving the central area unaffected. In contrast to the between-group alpha differences, this change was also reflected in a reduction of the RQA measures, and can also be observed in the right-temporal region. The reduction of the RP density and unpredictability of RR_τ can be interpreted as a system that does not return to previous states. The beta band has been associated with the preservation of the current brain state during a working memory task [44] and has been found to reflect diminished synchronization in AD [45]. Our results could suggest that it is also involved in state maintenance during rest, which seems to be impaired in MCI and AD.

Differences in the delta and gamma bands were only found between controls and patients with MCI using KLD. Previous studies found a reduction in irregularity and complexity in the delta band [6]. An increase in delta EEG power has also been reported in MCI patients [46]. Our results suggest that a slight increase in delta non-stationarity in the central region appears during the early stages of dementia due to AD. However, this increase is not reflected in any changes to the normal recurrence structure of this frequency band, perhaps due to this increase not being significant enough to alter the normal recurrence structure of oscillatory activity. It has been stated that gamma oscillations decrease as part of the normal aging process, supporting their possible relevance for MCI and AD [47]. Gamma activity has not been widely studied in MCI and AD by means of EEG, as this band displays an unfavorable signal-to-noise ratio [48]. However, it has been shown that gamma synchronization is disrupted in AD, suggesting an impairment in neural information processing [48]. Furthermore, and more in line with our results, a reduction in gamma functional connectivity in patients with MCI was previously reported [49]. The aforementioned studies were focused on functional connectivity, but our results suggest that the increase in non-stationarity in patients with MCI may reflect an early disruption of normal locally activated gamma activity that is not present in AD. This may suggest that gamma disruption could also be a sign of early neurodegeneration.

Both global non-stationarity and the unpredictability of RR_τ were increased in the MCI group compared to controls. These results are particularly interesting, since they suggest that higher frequency non-stationarity patterns are dominant in the MCI group, while global RQA unpredictability in this group is closer to the patterns found in lower frequencies. The results for KLD further support the hypothesis of an impairment in neuronal disinhibition in MCI patients, as excessive neuronal activity leading to the highest non-stationarity level of all three groups can be observed in a wide frequency spectrum [40]. The observed $ENTR_{RR}$ increase in MCI subjects in the global band was not coupled with a statistically significant increase in RR_τ, which indicates that EEG recurrences are more unpredictable in MCI subjects than in controls in the wide 1-70 Hz band, but not significantly denser. This could suggest that global EEG activation in MCI subjects returns to previous states a similar number of times than controls, but these recurrences happen in a more irregular and unpredictable way. This could perhaps be linked to the aforementioned increase in non-stationarity and imply that early neurodegeneration can be observed in the overall EEG activity. However, the study of the dynamic EEG properties in AD patients benefits more from the fine-grained analysis of frequency band separation.

It has been found that the overall average duration of microstates in AD is significantly shorter than that of healthy controls [50]. Furthermore, it has been suggested that abnormalities in resting-state preclinical AD can be also be detected [50]. $ENTR_{RR}$ revealed that there were significant differences in the global unpredictability of the recurrence structure in patients with MCI and AD compared to controls. The concept of microstates and their dynamic changes is intrinsically linked to the grand-average dynamic recurrent behavior of all the EEG channels. EEG microstates have been interpreted as maps generated by coordinated activity of neural assemblies, while their transitions express the activation of different brain networks [50]. As previously stated, the increase in global recurrence unpredictability observed in patients with MCI and AD means that EEG activity does not remain in a similar state for long, but does return to similar states often. In contrast, healthy controls show less dynamic recurrent behavior, which could mean that their EEG states remain stable for longer times. This is further supported by KLD showing that global EEG activity is more non-stationary in MCI and AD than in healthy aging.

5.2. Differences in local activation patterns between measures

The second research question was whether different methods of measuring the dynamic properties of locally-activated EEG activity (CWT and RQA) could reveal distinct disease-induced abnormalities in cortical oscillatory activity. Our results indicate that both methods share information. On one hand, the time-frequency approach reveals specific patterns in the delta, alpha and gamma bands. On the other hand, RQA presents beta-1 patterns of decreased RP density and unpredictability in MCI patients that the CWT-derived KLD fails to show. This could suggest that each of the approaches can extract complementary information. Perhaps KLD is more appropriate to characterize the evolution of the spectral content of the EEG thanks to the variable resolution of the CWT. The RQA measures might be better suited to characterize temporal transitions and changing dynamics of the state recurrence of the neural system. However, alternative explanations should be considered: KLD could simply be more sensitive to alterations to normal EEG oscillatory activity than RQA measures. This could be due to the embedding parameters that have to be chosen in RPs, which could obfuscate the true recurrence structure of the system, generating spurious correlations [15]. We tried to limit

this by optimizing the parameters in a previous study [13]; however, there are no optimal values for the embedding dimension and delay, and noise will always have an effect to the detriment of real dynamics [51].

The grand-average values of $ENTR_{RR}$ and MED_{RR} showed different distributions compared to one another. However, the statistically significant differences displayed very similar spatial patterns throughout all frequencies, with the MED_{RR} differences being less significant in general. This can be explained as a direct consequence of the definition of $ENTR_{RR}$. A RP with many disruptions to the recurrence structure (white diagonal bands) will have many points where RR_τ is close to 0, thus leading to a lower MED_{RR} value. This will also decrease $ENTR_{RR}$, as the unpredictability of the system will go down. It is worth pointing out, however, that $ENTR_{RR}$ and MED_{RR} do not necessarily have to show similar patterns. For example, an extremely highly populated RP would have a MED_{RR} of almost 1 but its $ENTR_{RR}$ would be close to 0. MED_{RR} displayed localized significant differences in the left hemisphere that $ENTR_{RR}$ failed to show, which indicates that the information that MED_{RR} provides may not be entirely redundant. What our results suggest is that MCI and AD affect recurrence density and unpredictability in a similar way: the recurrence structure of resting-state EEG activity of MCI and AD patients is both more dense and more unpredictable in the theta band, while the opposite is true in the beta band. This means that when the recurrence density increases for MCI and AD patients, it does so in a non-regular fashion across the RP. When the recurrence density decreases, the RP is more homogeneously populated.

5.3. Evolution of locally-activated dynamic properties through the MCI-AD continuum

While MCI has been considered a prodromal stage of AD [5], there is currently no consensus on whether it actually is a transitional state between normal aging and AD or simply represents a state of increased risk of developing AD [52]. Our results provide interesting information on this hypothesis. RQA measures in the theta and beta-2 bands reveal patterns of statistical differences between controls and patients with MCI that become more significant in AD. KLD shows similar results in the alpha band, except the patterns become less significant when comparing with AD patients. Interestingly, delta, alpha and gamma KLD in MCI show patterns of statistical differences with controls that either disappear or become less marked in AD patients. As previously discussed, the results in the alpha band are especially interesting for the hypothesis that MCI and AD constitute a continuum. Our results support the notion that MCI patients display abnormally high activity as a sign of AD pathogenesis [40]. The alpha activity is less non-stationary than the one found in healthy controls, indicating that the neuronal oscillations are more structured than that of normal aging. This could mean that, during the early stages of AD, a cascade of increasing stationary activity that alters the normal state switching develops. This increased activity may not be a compensatory mechanism but a consequence of impaired inhibitory neurons, which might be linked to the development of amyloid plaques [40]. This could explain why the activity becomes more homogeneous, as opposed to the normal, more dynamic behavior. Later, when MCI has progressed to AD, this increased activity in the alpha band disappears and abnormal oscillations start becoming more present in the theta band, as has been reported in other studies [53, 36].

Our findings support the notion that alterations of dynamic resting-state EEG activity might be reflective of the evolution of neurodegeneration with the progression of AD. It has been found that the regions conforming the default mode network (DMN) correspond to a high degree with high aerobic glycolysis regions [54]. It has been speculated that the elevated aerobic glycolysis in these areas acts as a defensive system against Aβ accumulation during aging, since drugs that increase aerobic glycolysis were shown to enhance neuronal survival in mouse AD models [54].The high activation during rest found in patients with MCI could be related to the progressive deterioration of this pre-emptive protective mechanism. After the mechanism wears out with the progression of the disease, the areas in the DMN would become more susceptible to neurodegeneration, leading to more pronounced cognitive impairment.

5.4. Limitations and future research lines

The present study has several limitations that should be considered. Firstly, three parameters (threshold ε, embedding dimension m, and delay τ) have to be carefully selected for an appropriate, artifact-free construction of RPs. While we tried to optimize these parameters with well-established methods, such as the mutual information function and the nearest neighbors algorithm, there is no set optimal method specific to this problem [55]. A possible alternative that could be used in future studies are unthresholded RPs, which are based on the correlation sum instead of a threshold [15]. Finding optimal values for embedding dimension m, and delay τ is an interesting future research line, as it could lead to a more optimized computation of the RQA measures which would enable a more reliable comparison between the groups.

Secondly, further research is needed to confirm whether the patients with MCI in our database

progress to AD at a later date. As it stands now, there may be two distinct subgroups of patients with MCI, one closer to AD and another to controls, which could explain the in-between behavior found in theta and beta. The results for KLD in the alpha, delta and gamma bands could support the notion of MCI being a distinct subgroup, as patients with AD did not show alterations in locally-activated oscillatory activity compared to controls. However, the aforementioned theta and beta behavior could support the notion of MCI and AD being a continuum. Nonetheless, it would be interesting to perform a longitudinal study when the information is available to gain a deeper understanding of the neural changes in MCI. This could help to arrive at a conclusion on whether MCI and AD are part of a continuum or distinct entities.

Finally, while this study focused on the dynamic properties of resting-state EEG activity, future research should focus on assessing whether the altered recurrence structures found in single channels for patients with MCI and AD could also be found in network state switching. To this end, RPs could be used to determine data-driven sliding windows in which the system is in the same state [56]. The results from the RQA measures suggest that state switching might be altered in the theta and beta bands for patients with MCI and AD. This is an especially interesting research line that we wish to pursue in future studies.

6. Conclusions

Our findings suggest that dynamic EEG resting-state behavior is abnormal in patients with MCI and AD, both in the level of non-stationarity and the recurrence structure, with the observed alterations being frequency-dependent. Furthermore, alterations to the normal recurrence structure suggest that MCI and AD induce changes to the normal state switching of the cortical activity.

We also showed that approaching the characterization of EEG dynamics by means of different methodologies, based on the CWT and RPs is useful to reveal specific patterns of anomalous behavior. The results showed that alterations to non-stationarity in specific frequency bands might not be accompanied by aberrant recurrence structures and vice-versa. This could mean that these approaches might be useful as potential complementary biomarkers for MCI and AD.

7. Acknowledgements

This research was supported by 'European Regional Development Fund' (FEDER) and 'Ministerio de Ciencia, Innovación y Universidades' under projects PGC2018-098214-A-I00 and DPI2017-84280-R, the 'European Commission' and FEDER under project 'Análisis y correlación entre el genoma completo y la actividad cerebral para la ayuda en el diagnóstico de la enfermedad de Alzheimer' ('Cooperation Programme Interreg V-A Spain-Portugal, POCTEP 2014-2020'), and by CIBER-BBN (ISCIII) co-funded with FEDER funds. P. Núñez was in receipt of a predoctoral scholarship 'Ayuda para contratos predoctorales para la Formación de Profesorado Universitario (FPU)' grant from the 'Ministerio de Educación, Cultura y Deporte' (FPU17/00850). V. Barroso-García was in receipt of a 'Ayuda para financiar la contratación predoctoral de personal investigador' grant from the Consejería de Educación de la Junta de Castilla y León and the European Social Fund.

References

[1] Babiloni C, Lizio R, Marzano N, Capotosto P, Soricelli A, Triggiani A I, Cordone S, Gesualdo L and Del Percio C 2015 Brain neural synchronization and functional coupling in Alzheimer's disease as revealed by resting state EEG rhythms *International Journal of Psychophysiology* **103** 88–102 ISSN 18727697

[2] Tognoli E and Kelso J A S 2014 The Metastable Brain *Neuron* **81** 35–48 ISSN 08966273

[3] Michel C M and Koenig T 2018 EEG microstates as a tool for studying the temporal dynamics of whole-brain neuronal networks: A review *NeuroImage* **180** 577–593 ISSN 10959572 (*Preprint* 0406177)

[4] Dauwels J, Vialatte F and Cichocki A 2010 Diagnosis of Alzheimer's disease from EEG Signals: where are we standing? *Current Alzheimer Research* **7** 487–505 ISSN 15672050

[5] Petersen R C 2004 Mild cognitive impairment as a clinical entity and treatment target. *Archives of Neurology* **62** 1160–1163; discussion 1167 ISSN 0003-9942

[6] Poza J, Gómez C, García M, Tola-Arribas M A, Carreres A, Cano M and Hornero R 2017 Spatio-temporal fluctuations of neural dynamics in mild cognitive impairment and Alzheimer's disease *Current Alzheimer Research* **14** 924–936 ISSN 15672050

[7] Poza J, Gómez C, García M, Corralejo R, Fernández A and Hornero R 2014 Analysis of neural dynamics in mild cognitive impairment and Alzheimer's disease using wavelet turbulence *Journal of Neural Engineering* **11** 026010 ISSN 1741-2560

[8] Gómez C, Juan-Cruz C, Poza J, Ruiz-Gómez S J, Gomez-Pilar J, Núñez P, García M, Fernández A and Hornero R 2018 Alterations of Effective Connectivity Patterns in Mild Cognitive Impairment: An MEG Study *Journal of Alzheimer's Disease* **65** 843–854 ISSN 13872877

[9] O'Neill G C, Tewarie P, Vidaurre D, Liuzzi L, Woolrich M W and Brookes M J 2018 Dynamics of large-scale electrophysiological networks: A technical review *NeuroImage* **180** 559–576 ISSN 10538119

[10] Zbilut J P and Webber C L 2006 Recurrence Quantification Analysis *Wiley Encyclopedia of Biomedical Engineering* 2 ISBN 978-3-319-07154-1

[11] Blanco S, Garcia H, Quiroga R Q, Romanelli L and Rosso O A 1995 Stationarity of the EEG series *IEEE Engineering in Medicine and Biology Magazine* **14** 395–399 ISSN 07395175

[12] Rosso O A, Martin M T, Figliola A, Keller K and Plastino A 2006 EEG analysis using wavelet-based information tools

Journal of Neuroscience Methods **153** 163–182 ISSN 01650270

[13] Núñez P, Poza J, Gómez C, Rodríguez-González V, Ruiz-Gómez S J, Maturana-Candelas A and Hornero R 2019 Characterizing Non-stationarity in Alzheimer's Disease and Mild Cognitive Impairment by Means of Kullback-Leibler Divergence *Biosystems and Biorobotics* pp 574–578 ISSN 21953570

[14] Núñez P, Poza J, Gómez C, Rodríguez-González V, Ruiz-Gómez S, Maturana-Candelas A and Hornero R 2019 Characterization of EEG resting-state activity in Alzheimer's disease by means of recurrence plot analyses *Proceedings of the 41st Annual International Conference of the IEEE Engineering in Medicine and Biology Society Conference* pp 5786–5789

[15] Marwan N, Carmen Romano M, Thiel M and Kurths J 2007 Recurrence plots for the analysis of complex systems *Physics Reports* **438** 237–329 ISSN 03701573

[16] Núñez P, Poza J, Bachiller A, Gomez-Pilar J, Lubeiro A, Molina V and Hornero R 2017 Exploring non-stationarity patterns in schizophrenia: Neural reorganization abnormalities in the alpha band *Journal of Neural Engineering* **14** 1–12 ISSN 17412552

[17] Tong S, Li Z, Zhu Y and Thakor N V 2007 Describing the nonstationarity level of neurological signals based on quantifications of time-frequency representation *IEEE Transactions on Biomedical Engineering* **54** 1780–1785 ISSN 0018-9294

[18] McKhann G, Knopman D S, Chertkow H, Hymann B, Jack C R, Kawas C, Klunk W, Koroshetz W, Manly J, Mayeux R, Mohs R, Morris J, Rossor M, Scheltens P, Carrillo M, Weintrub S and Phelphs C 2011 The diagnosis of dementia due to Alzheimer's disease: Recommendations from the National Institute on Aging- Alzheimer's Association workgroups on diagnostic guidelines for Alzheimer's disease *Alzheimers Dementia* **7** 263–269 ISSN 1552-5279 (*Preprint* `NIHMS150003`)

[19] Albert M S, DeKosky S T, Dickson D, Dubois B, Feldman H H, Fox N C, Gamst A, Holtzman D M, Jagust W J, Petersen R C, Snyder P J, Carrillo M C, Thies B and Phelps C H 2011 The diagnosis of mild cognitive impairment due to Alzheimer's disease: Recommendations from the National Institute on Aging-Alzheimer's Association workgroups on diagnostic guidelines for Alzheimer's disease *Alzheimer's and Dementia* **7** 270–279 ISSN 15525260 (*Preprint* `NIHMS150003`)

[20] Núñez P, Poza J, Gomez C, Rodríguez-González V, Hillebrand A, Tola-Arribas M Á, Cano M and Hornero R 2019 Characterizing the fluctuations of dynamic resting-state electrophysiological functional connectivity: Reduced neuronal coupling variability in mild cognitive impairment and dementia due to Alzheimer's disease *Journal of Neural Engineering* ISSN 1741-2560

[21] Roach B J and Mathalon D H 2008 Event-related EEG time-frequency analysis: An overview of measures and an analysis of early gamma band phase locking in schizophrenia *Schizophrenia Bulletin* **34** 907–926 ISSN 05867614

[22] Rioul O and Vetterli M 1991 Wavelets and signal processing *IEEE Signal Processing Magazine* **8** 14–38 ISSN 1053-5888

[23] Tallon-Baudry C, Bertrand O, Delpuech C and Pernier J 1996 Stimulus Specificity of Phase-Locked and Non-Phase-Locked 40 Hz Visual Responses in Human *The Journal of Neuroscience* **16** 4240–4249 ISSN 0270-6474

[24] Samar V J, Bopardikar A, Rao R and Swartz K 1999 Wavelet analysis of neuroelectric waveforms: a conceptual tutorial *Brain and Language* **66** 7–60 ISSN 0093934X

[25] Bachiller A, Poza J, Gómez C, Molina V, Suazo V and Hornero R 2015 A comparative study of event-related coupling patterns during an auditory oddball task in schizophrenia *Journal of Neural Engineering* **12** 016007 ISSN 1741-2560

[26] Torrence C and Compo G P 1998 A practical guide to wavelet analysis *Bulletin of the American Meteorological Society* **79** 61–78 ISSN 00030007

[27] Webber C and Zbilut J 2005 Recurrence quantification analysis of nonlinear dynamical systems *Tutorials in Contemporary Nonlinear Methods for the Behavioral Sciences Web Book* pp 26–94

[28] Martín-González S, Navarro-Mesa J L, Juliá-Serdá G, Ramírez-Ávila G M and Ravelo-García A G 2018 Improving the understanding of sleep apnea characterization using Recurrence Quantification Analysis by defining overall acceptable values for the dimensionality of the system, the delay, and the distance threshold *PLoS ONE* **13** 1–35 ISSN 19326203

[29] Schinkel S, Dimigen O and Marwan N 2008 Selection of recurrence threshold for signal detection *European Physical Journal: Special Topics* **164** 45–53 ISSN 19516355

[30] Ouyang G, Li X, Dang C and Richards D A 2008 Using recurrence plot for determinism analysis of EEG recordings in genetic absence epilepsy rats *Clinical Neurophysiology* **119** 1747–1755 ISSN 13882457

[31] Heunis T, Aldrich C, Peters J M, Jeste S S, Sahin M, Scheffer C and de Vries P J 2018 Recurrence quantification analysis of resting state EEG signals in autism spectrum disorder - a systematic methodological exploration of technical and demographic confounders in the search for biomarkers *BMC Medicine* **16** 1–17 ISSN 17417015

[32] Marwan N, Wessel N, Meyerfeldt U, Schirdewan A and Kurths J 2002 Recurrence-plot-based measures of complexity and their application to heart-rate-variability data *Physical Review E - Statistical Physics, Plasmas, Fluids, and Related Interdisciplinary Topics* **66** 1–8 ISSN 1063651X

[33] Eckmann J P, Kamphorst S O and Ruelle D 1987 Recurrence Plots of Dynamical Systems *Europhysics Letters (EPL)* **4** 973–977 ISSN 0295-5075

[34] Freedman D and Diaconis P 1981 On the histogram as a density estimator: L2 theory *Zeitschrift für Wahrscheinlichkeitstheorie und Verwandte Gebiete* **57** 453–476 ISSN 05685230

[35] Benjamini Y and Hochberg Y 1995 Controlling the false discovery rate: a practical and powerful approach to multiple testing *Journal of the Royal Statistical Society* **57** 289–300 ISSN 00359246 (*Preprint* `95/57289`)

[36] Dauwels J, Srinivasan K, Ramasubba Reddy M, Musha T, Vialatte F B, Latchoumane C, Jeong J and Cichocki A 2011 Slowing and Loss of Complexity in Alzheimer's EEG: Two Sides of the Same Coin? *International Journal of Alzheimer's Disease* **2011** 1–10 ISSN 2090-0252

[37] Jeong J 2004 EEG dynamics in patients with Alzheimer's disease *Clinical Neurophysiology* **115** 1490–1505 ISSN 13882457

[38] Maestú F, Yubero R, Moratti S, Campo P, Gil-Gregorio P, Paul N, Solesio E, del Pozo F and Nevado A 2011 Brain Activity Patterns in Stable and Progressive Mild Cognitive Impairment During Working Memory as Evidenced by Magnetoencephalography *Journal of Clinical Neurophysiology* **28** 202–209 ISSN 0736-0258

[39] Gaubert S, Raimondo F, Houot M, Corsi M C, Naccache L, Diego Sitt J, Hermann B, Oudiette D, Gagliardi G, Habert M O, Dubois B, De Vico Fallani F, Bakardjian H, Epelbaum S, Bakardjian H, Benali H, Bertin H, Bonheur

J, Boukadida L, Boukerrou N, Cavedo E, Chiesa P, Colliot O, Dubois B, Dubois M, Epelbaum S, Gagliardi G, Genthon R, Habert M O, Hampel H, Houot M, Kas A, Lamari F, Levy M, Lista S, Metzinger C, Mochel F, Nyasse F, Poisson C, Potier M C, Revillon M, Santos A, Andrade K S, Sole M, Surtee M, de Schotten M T, Vergallo A and Younsi N 2019 EEG evidence of compensatory mechanisms in preclinical Alzheimer's disease *Brain* **142** 1497–1500 ISSN 0006-8950

[40] de Haan W, Mott K, van Straaten E C, Scheltens P and Stam C J 2012 Activity Dependent Degeneration Explains Hub Vulnerability in Alzheimer's Disease *PLoS Computational Biology* **8** ISSN 1553734X (*Preprint* `journal.pcbi.1002582`)

[41] Palop J J and Mucke L 2010 Amyloid-β–induced neuronal dysfunction in Alzheimer's disease: from synapses toward neural networks *Nature Neuroscience* **13** 812–818 ISSN 1097-6256

[42] Haense C, Kalbe E, Herholz K, Hohmann C, Neumaier B, Krais R and Heiss W D 2012 Cholinergic system function and cognition in mild cognitive impairment *Neurobiology of Aging* **33** 867–877 ISSN 01974580

[43] Quiroz Y T, Budson A E, Celone K, Ruiz A, Newmark R, Castrillón G, Lopera F and Stern C E 2010 Hippocampal hyperactivation in presymptomatic familial Alzheimer's disease *Annals of Neurology* **68** 865–875 ISSN 03645134

[44] Spitzer B and Haegens S 2017 Beyond the Status Quo: A Role for Beta Oscillations in Endogenous Content (Re)Activation *eneuro* **4** ENEURO.0170–17.2017 ISSN 2373-2822

[45] Stam C J, van der Made Y, Pijnenburg Y A L and Scheltens P 2003 EEG synchronization in mild cognitive impairment and Alzheimer's disease *Acta Neurologica Scandinavica* **108** 90–96 ISSN 0001-6314

[46] Babiloni C, Del Percio C, Lizio R, Noce G, Lopez S, Soricelli A, Ferri R, Pascarelli M T, Catania V, Nobili F, Arnaldi D, Famà F, Aarsland D, Orzi F, Buttinelli C, Giubilei F, Onofrj M, Stocchi F, Vacca L, Stirpe P, Fuhr P, Gschwandtner U, Ransmayr G, Garn H, Fraioli L, Pievani M, Frisoni G B, D'Antonio F, De Lena C, Güntekin B, Hanoğlu L, Başar E, Yener G, Emek-Savaş D D, Triggiani A I, Franciotti R, Taylor J P, De Pandis M F and Bonanni L 2018 Abnormalities of resting state cortical EEG rhythms in subjects with mild cognitive impairment due to Alzheimer's and Lewy body diseases *Journal of Alzheimer's Disease* **62** 247–268 ISSN 13872877

[47] Herrmann C S and Demiralp T 2005 Human EEG gamma oscillations in neuropsychiatric disorders *Clinical Neurophysiology* **116** 2719–2733 ISSN 13882457

[48] Stam C J, Van Cappellen van Walsum A M, Pijnenburg Y A, Berendse H W, De Munck J C, Scheltens P and Van Dijk B W 2002 Generalized synchronization of MEG recordings in Alzheimer's disease: Evidence for involvement of the gamma band *Journal of Clinical Neurophysiology* **19** 562–574 ISSN 07360258

[49] Gomez C, Stam C, Hornero R, Fernandez A and Maestu F 2009 Disturbed beta band functional connectivity in patients With mild cognitive impairment: An MEG study *IEEE Transactions on Biomedical Engineering* **56** 1683–1690 ISSN 0018-9294

[50] Khanna A, Pascual-Leone A, Michel C M and Farzan F 2015 Microstates in resting-state EEG: Current status and future directions *Neuroscience & Biobehavioral Reviews* **49** 105–113 ISSN 01497634

[51] Zbilut J P, Zaldivar-Comenges J M and Strozzi F 2002 Recurrence quantification based Liapunov exponents for monitoring divergence in experimental data *Physics Letters A* **297** 173–181 ISSN 03759601

[52] Stephan B C M, Hunter S, Harris D, Llewellyn D J, Siervo M, Matthews F E and Brayne C 2012 The neuropathological profile of mild cognitive impairment (MCI): a systematic review *Molecular Psychiatry* **17** 1056–1076 ISSN 1359-4184

[53] Uhlhaas P J and Singer W 2006 Neural synchrony in brain disorders: relevance for cognitive dysfunctions and pathophysiology *Neuron* **52** 155–168 ISSN 08966273

[54] Sheline Y I and Raichle M E 2013 Resting State Functional Connectivity in Preclinical Alzheimer's Disease *Biological Psychiatry* **74** 340–347 ISSN 00063223

[55] Zbilut J P, Thomasson N and Webber C L 2002 Recurrence quantification analysis as a tool for nonlinear exploration of nonstationary cardiac signals *Medical Engineering & Physics* **24** 53–60 ISSN 13504533

[56] Tewarie P, Liuzzi L, O'Neill G C, Quinn A J, Griffa A, Woolrich M W, Stam C J, Hillebrand A and Brookes M J 2019 Tracking dynamic brain networks using high temporal resolution MEG measures of functional connectivity *NeuroImage* **200** 38–50 ISSN 10538119